AEDC-TR-68-88

cy'

DETERMINATION OF TRANSIENT GAS CONSTITUENT CONCENTRATIONS UTILIZING A HIGH ENERGY ELECTRON BEAM

R. G. Whetsel

ARO, Inc.

May 1968

VON KÁRMÁN GAS DYNAMICS FACILITY
ARNOLD ENGINEERING DEVELOPMENT CENTER
AIR FORCE SYSTEMS COMMAND
ARNOLD AIR FORCE STATION, TENNESSEE

NOTICES

DETERMINATION OF TRANSIENT GAS CONSTITUENT
CONCENTRATIONS UTILIZING A ʻ
HIGH ENERGY ELECTRON BEAM

R. G. Whetsel

ARO, Inc.

FOREWORD

The work reported herein was sponsored by the Arnold Engineering Development Center (AEDC), Air Force Systems Command (AFSC), Arnold Air Force Station, Tennessee, under Program Element 6241003F, Project 7778, Task 777807.

The results of research presented were obtained by ARO, Inc. (a subsidiary of Sverdrup & Parcel and Associates, Inc.), contract operator of AEDC, AFSC, under Contract AF40(600)-1200. The work was conducted under ARO Project No. VJ3708 from November 1, 1966, to April 1, 1967. This material was presented to the University of Tennessee as a thesis in partial fulfillment of the requirements for the degree of Master of Science. The manuscript was submitted for publication on March 25, 1968.

This technical report has been reviewed and is approved.

Marshall Kingery
Research Division
Directorate of Plans
  and Technology

Edward R. Feicht
Colonel, USAF
Director of Plans
  and Technology

ABSTRACT

In order to determine the available test time in a helium driven shock tunnel, an interface detection system has been developed to indicate the arrival of helium driver gas at the test section. This is done by exciting the gas at the test section with a high energy electron beam and spectroscopically analyzing the resulting fluorescence to determine the helium concentration. Relative values of helium and air emission intensities are calculated and compared with experimental data from both static and transient gas mixtures.

CONTENTS

ILLUSTRATIONS

CHAPTER I
TRANSIENT GAS CONCENTRATIONS IN SHOCK TUNNELS

In the process of determining the aerodynamic flow parameters in the test section of a shock tunnel, it is necessary to determine the duration of usable test flow as limited by the arrival of the test gas (driven tube gas) - driver gas interface. This investigation will deal with a helium-air interface.

A diagram of the shock tunnel is shown in Figure 1. A high velocity, low density test flow is generated by precharging the driven tube to a pressure which will yield prescribed test section conditions. The driver section is then pressurized until a diaphragm separating the two sections is ruptured which initiates a compression shock in the driven tube gas. When this pressure rises sufficiently, a second diaphragm between the driven tube and the previously evacuated dump tank ruptures, causing a high velocity, low density flow to pass through the test section area. The parameters of pressure, diaphragm thickness, tube lengths, and nozzle dimensions are predicted from shock tunnel practice. This thesis deals only with the analysis, development, and evaluation of the electron beam interface detection system. For a discussion of the shock tunnel parameters, see Hertzberg and others (1).[1]

---

[1]Numbers in parentheses refer to similarly numbered references in the bibliography.
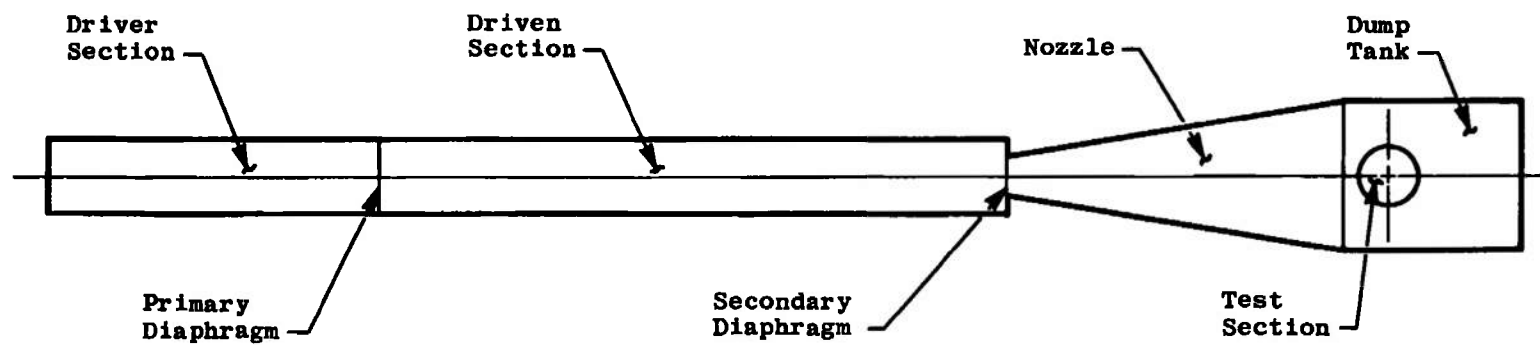
Fig. 1 Diagram of a Shock Tunnel

There are at least three requirements which any interface detection technique must satisfy. First, the predicted usable test flow time is on the order of a few hundred microseconds; therefore, the method selected must have the capability of tens of microseconds response time. Second, it is not known whether the driver gas arrives as a well defined surface or if there is a region of diffused mixing comparable to the test time; therefore, the interface detection system must indicate the time resolved percentage concentration of driver gas. Finally, it is desirable to be able to measure the flow concentration at a given position in the flow; therefore, the technique should have the capability of nearly point resolution.

Kaegi and Muntz (2) discuss the above points for the conditions of their study of interface arrival. Their work consisted of monitoring the density of nitrogen and helium as measured by the electron beam technique described by Muntz and Marsden (3). The interface was identified with a decrease in nitrogen density or an increase in helium density. The two gases were monitored independently on separate tunnel runs.

Copper, Miller, and Hameetman (4) and Bird, Martin, and Bell (5) obtained data on both helium and hydrogen driver gas interface arrival. Their method consisted of four fast acting sampling probes which were open at four different periods over about ten milliseconds of apparent flow time. The total open time was about two milliseconds. In this manner four samples representing average mixtures were obtained. These samples were subsequently analyzed by gas chromatographic methods.

This work was undertaken because a valid measure of run time is needed and the earlier data were not considered sufficiently accurate or complete for making predictions of shock tunnel performance.

Chapter II gives an introduction to electron beam diagnostics and a description of the electron beam diagnostic system used to take the data in Chapter IV. A theoretical expression for the relative intensities of electron beam excited radiation in helium-air gas mixtures is derived in Chapter III. Experimental data for both static and transient helium-air gas mixtures are presented in Chapter IV.

CHAPTER II
ELECTRON BEAM GAS DIAGNOSTICS

I. THE ELECTRON BEAM GAS DIAGNOSTIC TECHNIQUE!

A totally satisfactory method for determining the unperturbed
parameters in a high velocity (30,000 feet/sec), low density (approximately five Torr at 300°K maximum) aerodynamic flow has not been
offered. Although tedious, spectroscopic techniques are particularly
attractive since they can be employed without causing any disturbance
in the gas during the time of measurement. Both emission and absorption spectroscopy can be considered. However, at the conditions given
above the gas does not emit or absorb a sufficient amount of radiation
for quantitative measurements.

The high energy (10-50 KV) electron electron beam holds some
promise. By directing a well-collimated beam of electrons into the
flow the gas is caused to fluoresce within the beam volume. Inelastic
collisions of the electrons with the gas molecules result in the
excitation of the gas molecules. In many common gases such as nitrogen,
helium, argon, carbon dioxide, hydrogen, and others some of the energy
resulting from subsequent spontaneous de-excitations of the molecules
is radiated in the easily-handled optical spectrum [approximately 2000
$\overset{o}{A}$ (one Angstrom $\overset{o}{A}$ equals 10^{-10} meters) to 10^4 $\overset{o}{A}$ wavelength]. Spectroscopic analysis of this radiation has been used to make measurements

of several flow parameters.

Schumaker and Gadamer (6) used the electron beam to measure nitrogen density below 100 millitorr by detecting the change in beam radiation intensity with density at a known beam current. They found a linear relationship in this range. A well-collimated beam and an accurate beam current measurement are critical to this technique.

Muntz (7) used the relative line intensity method described by Hertzberg (8) to measure the vibrational and rotational temperature of the unperturbed gas. Since the relaxation times for rotational and translational temperatures are comparable, this technique offers a means of obtaining the temperature for use in thermodynamic and aerodynamic theoretical analyses. Measurements of vibrational temperature provide a determination of the degree of non-equilibrium.

Muntz (9) made use of the Doppler broadening of the beam excited emission lines to obtain data on the molecular velocity distributions in a low density gas. This was done by measuring the Doppler width of the 5016 $\overset{o}{A}$ helium line.

The electron beam therefore provides a means of exciting a selected portion of a low density, high velocity flow in such a manner that optical spectroscopic techniques can be used to make measurements of the undisturbed free stream parameters of the flow.

The electron beam flow diagnostic technique has several pitfalls. The successful application of the electron beam excitation technique to any particular flow field investigation depends on an approximate knowledge of the flow parameters and the specific operational

limitations. The electron beam generating system must provide a well collimated, stable stream of electrons before conclusions can be drawn with regard to particular regions of the flow. This is especially true in density measurements. Care must be taken that the electron beam hardware and optics do not produce disturbances near the point of measurement. An often encountered problem is background luminosity due to flow contamination. Valid data can only be obtained when the radiation accepted by the spectrometer from sources other than the beam are reduced to an acceptable level. The level of acceptable background radiation is directly dependent on the absolute intensity of beam radiation. In general, the higher the density and beam current the greater the background intensity that can be tolerated.

Another area which must be considered is the degree to which the flow conditions and the assumed excitation and de-excitation mechanisms due to the electron beam comply with the actual conditions. Muntz, Abel, and Maquire (10), Muntz (7), and Petrie (11) give a quite exhaustive commentary on this topic.

II. THE ELECTRON BEAM SYSTEM

The development of an electron beam generating system and associated optical detection system poses a myriad of problems. A diagram of the system used for taking data in the eight foot diameter test section of Tunnel "J" at Arnold Engineering Development Center is shown in Figure 2. A television type electron gun with magnetic focusing was used to generate the electron beam. An early attempt with
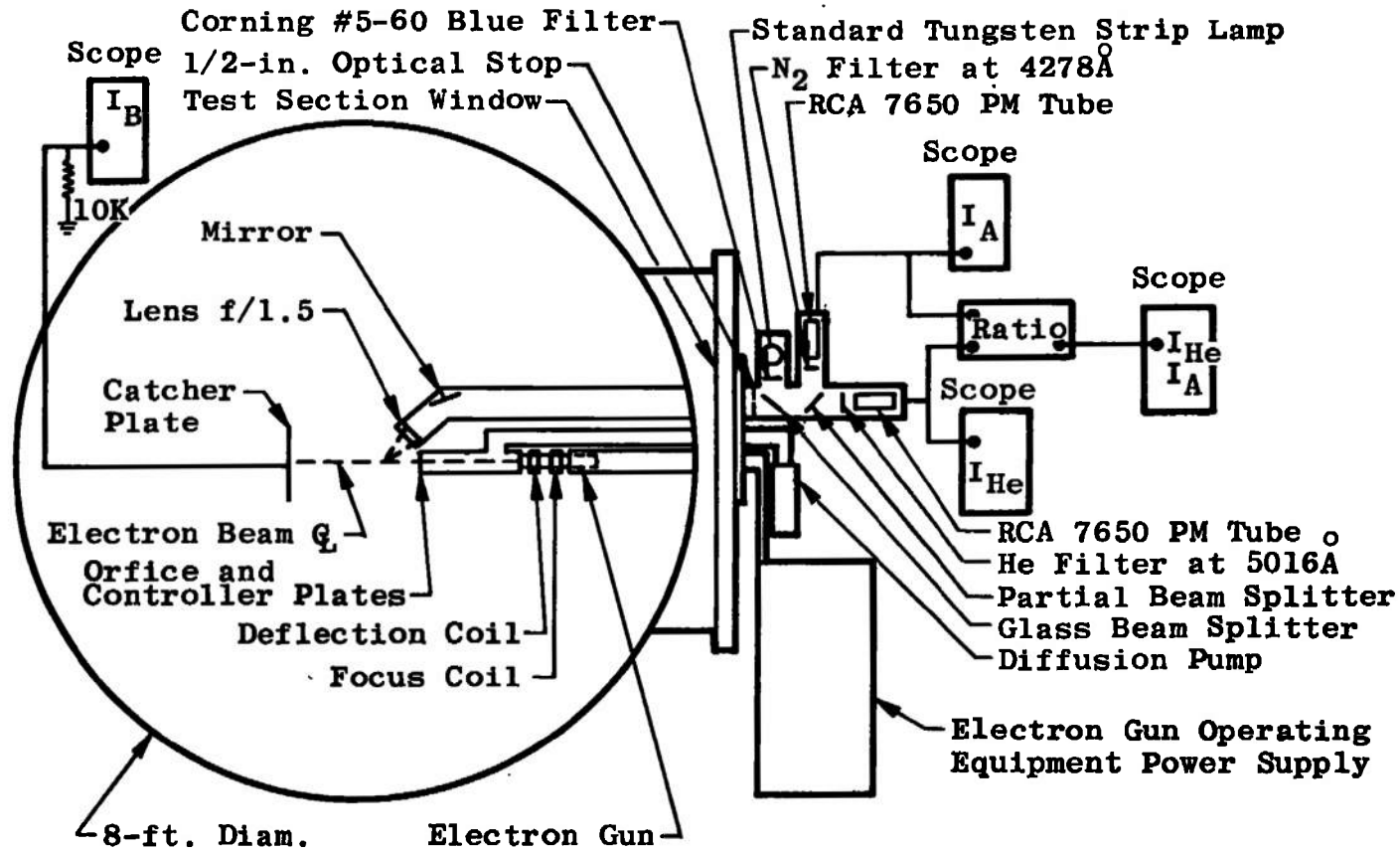
Fig. 2 View of Electron Beam System in Test Section, Looking Downstream

electrostatic focusing was terminated due to the difficulty of design-
ing a power supply with the cathode operated at high voltage rather
than near ground as in conventional circuits. These electron guns are
capable of operating at 20 KV while delivering four to five milliam-
peres of cathode current. The filaments are designed for six volt
excitation but they were routinely operated at eighteen volts. While
this reduced the lifetime of the gun it provided additional emission
and allowed operation at pressures above the normal operating range.
In order to provide a steady beam care must be taken to provide low
ripple direct current power supplies throughout the electron beam
generation system.

It is necessary that the pressure in the electron gun be 3 x
10^{-4} Torr or less for acceptable operation. In order to maintain this
pressure while the pressure in the test section may be as high as one
Torr for a few milliseconds, it is necessary to use a dynamic pumping
system. This technique requires firing the beam through a small orifice
across which the necessary pressure differential can be maintained by
continuous pumping. The system in Figure 2 uses a 0.050 inch diameter
orifice with a sixty liter per second diffusion pump. A pressure of
150 millitorr can be maintained easily in a small test section enclos-
ing the electron gun exit orifice with the electron beam in operation.
Satisfactory operation has been obtained with transient flows of a few
milliseconds in duration up to densities equivalent to 700 microns at
room temperature.

Passing a major portion of an electron beam which is one to two

millimeters in diameter through a 0.050 inch (1.25 mm) diameter orifice places some rather stringent requirements on beam alignment. Static alignment of the beam is accomplished by varying the currents in an x-y deflection coil and maximizing the collected current. Dynamic realignment is done by a feedback control device developed by Froedge (12) which detects current resulting from misalignment of the beam and uses a voltage proportional to the time integral of this current to change the proper deflection coil current in the direction necessary to realign the beam. This control system has calculated response time of fifty microseconds.

Radiation from the beam is intercepted by a f/1.5 lens and transmitted outside the test section by a series of collimating lenses. At the partial beam splitter the light is separated into two beams. One beam is directed through a fifty $\overset{o}{A}$ half width interference filter centered on the 5016 $\overset{o}{A}$ atomic spectral line, which is prominent in helium electron beam excited radiation [see Sebachér (13)]. The second beam is directed through a seventeen $\overset{o}{A}$ half width interference filter centered at the 4278 $\overset{o}{A}$ bandhead of the (0,1) vibrational band in the first negative system of N_2^+, which is prominent in nitrogen electron beam radiation [see Sebacher (13)]. Both radiation outputs are detected with high gain RCA 7650 photomultipliers whose outputs are in turn displayed on oscilloscopes. In addition the photomultiplier outputs are fed into a diode type quarter-square multiplier connected as a divider. This device is discussed in Chapter IV. In this way the "in line" ratio of helium intensity divided by air (nitrogen) intensity is obtained.

A tungsten strip lamp was used as a radiation intensity standard. Radiation from the tungsten strip lamp was directed into the detector portion of the optics by a clear glass beam splitter. While the purpose of the standard lamp was to monitor the gain factors of the optical system over the several weeks that data were taken the calibration can also be used to make estimates of absolute intensity sensitivity.

A flat catcher plate about twelve inches in diameter and eighteen inches from the beam exit orifice was used to collect the electron beam. While it definitely did not provide a suitable measure of beam current for density measurements, it did give a measure of beam quality and continuity during the transient flow.

CHAPTER III
CALCULATION OF EXPECTED INTENSITIES

I. ESTIMATE OF PHOTON YIELD FROM ELECTRON BEAM INTERACTION WITH A GAS

The general equation for the intensity of a spectral line in emission is given in Herzberg (8):

$$I_{nm} = N_n \, h \, \nu_{nm} \, A_{nm}. \tag{1}$$

In this equation I_{nm} is the intensity of the radiation emitted into 4π steradians when the molecules or atoms of a gaseous ensemble decay from energy state n to energy state m, N_n is the number of molecules or atoms in energy state n, ν_{nm} is the frequency of the light, h is Planck's constant, and A_{nm} is the Einstein probability of a spontaneous emission. Values of A_{nm} are available for most of the prominent emission lines in the common gases. The frequency of the light can be determined directly. It remains to determine the number of molecules or atoms in the excited state n as a result of electron beam excitation.

Consider the energy level model in Figure 3. The following conditions will be assumed throughout the remainder of this analysis:

1. Only one lower or ground level ℓ will be considered. This is essentially true up to a few hundred degrees Kelvin above room temperature for most gases since the population of higher states is very low.
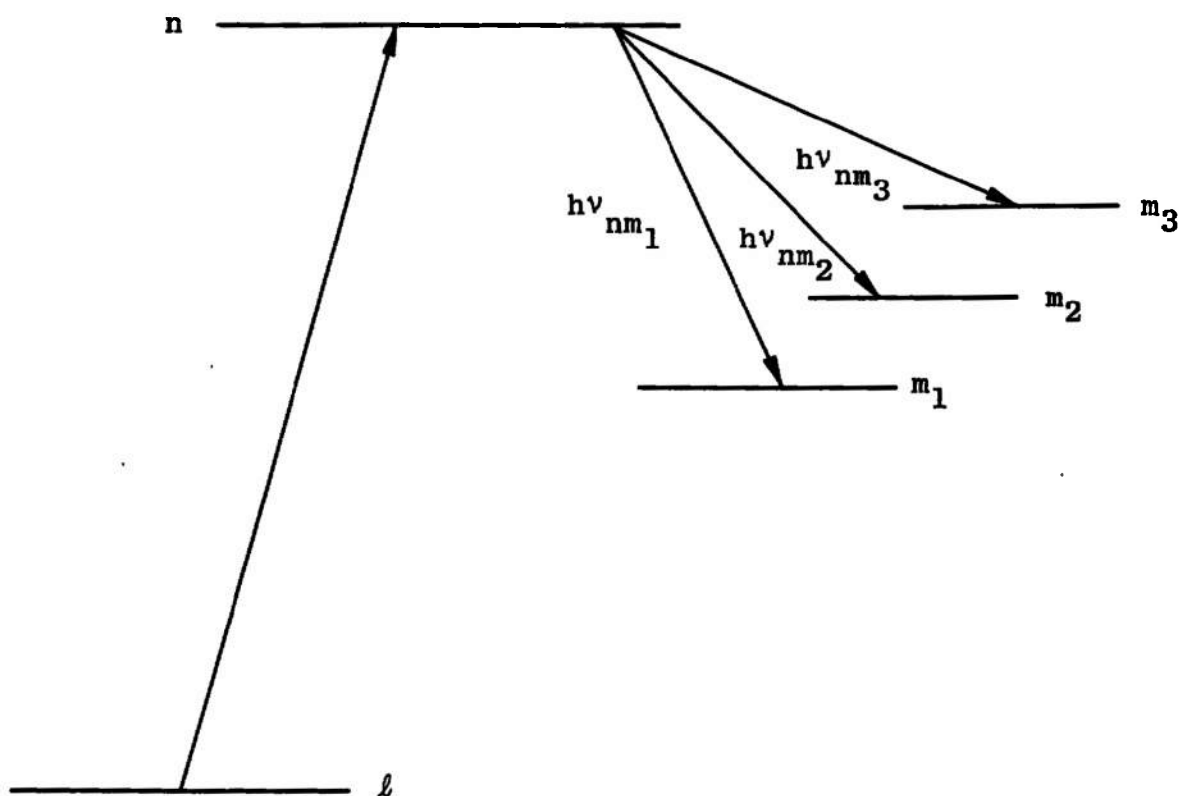
Fig. 3 Energy Level Model for Determining Electron
Beam Excited Emission Intensity of a Gas

2. The electron beam excitation is a direct excitation. There is no cascade population of the n excited energy level by higher levels. Also there are no excitations with intermediate stops at lower energy levels.

3. There are no collisional de-excitations from the excited state n.

The equation for the number of molecules or atoms being excited to the state n per unit volume and per unit time may be written,

$$N_{ex} = \left(\frac{I_b}{e \, A_b} \right) Q_{\ell n} \, N_\ell , \qquad (2)$$

$$\left\{ \frac{\text{molecules excited}}{\text{sec} \cdot \text{m}^3} \right\} = \left\{ \frac{\text{coul/sec}}{\text{coul} \cdot \text{m}^2} \right\} \left\{ \text{m}^2 \right\} \left\{ \frac{\text{molecules}}{\text{m}^3} \right\} ,$$

where I_b is the beam current, e is the electronic charge, A_b is the area of the beam, $Q_{\ell n}$ is the cross-section for excitation from state ℓ to state n, and N_ℓ is the number of molecules per unit volume in state ℓ. The equation for the number of molecules or atoms de-excited from state n may be written,

$$N_{DX} = \sum_m A_{nm} \, N_n . \qquad (3)$$

The decay times for spontaneous emission are on the order of 10^{-8} seconds for electric dipole transitions. Within a few decay times after the beam is turned on the number of excitations per second must equal the number of de-excitations per second.

$$\left(\frac{I_b}{e \, A_b} \right) Q_{\ell n} \, N_\ell = \sum_m A_{nm} \, N_n \; . \tag{4}$$

In this steady state condition N_n is a constant. Also $\sum_m A_{nm} = 1/\tau_n$, where τ_n is the mean lifetime of state n as defined in Herzberg (8).

$$N_n = \frac{I_b \, Q_{\ell n} \, N_\ell \, \tau_n}{e \, A_b} \; . \tag{5}$$

Substituting this result into Equation 1 gives

$$I_{nm} = \frac{h \, \nu_{nm} \, A_{nm} \, I_b \, Q_{\ell n} \, N_\ell \, \tau_n}{e \, A_b} \; . \tag{6}$$

The above expression gives the energy per unit volume per second radiated isotropically into 4π steradians due to the electron beam excitation of a single energy transition or a group of transitions which can conveniently be considered as a single transition. It is of interest to note that if it were valid to consider only one de-excitation transition the product of A_{nm} and τ_n would be one. In that case these two parameters would not appear in the expression for intensity.

In order to determine the absolute intensity available to a photodetector it is necessary to consider the geometry of the situation. Assuming an isotropic, homogeneous, optically thin medium the total power I_T radiated into 4π radians will be the product of the power radiated per unit volume and the volume of beam excited gas observed.

$$I_T = I_{nm} \, \ell_b \, A_b, \tag{7}$$

where ℓ_b is the length of beam observed. Substituting Equation 6 into Equation 7,

$$I_T = \frac{h \, \nu_{nm} \, A_{nm} \, I_b \, Q_{\ell n} \, N_\ell \ell_b \, \tau_n}{e} \quad . \tag{8}$$

The steradiancy intercepted by an optical system can be related to the system f number,

$$f = \frac{f_\ell}{D} \quad . \tag{9}$$

Where f is the system f number, D is the lens stop diameter, and f_ℓ is the focal length of the optical component in the system with the maximum f number. The intercepted solid angle Ω is

$$\Omega = \frac{A}{d^2} \quad . \tag{10}$$

Where A is the collector lens area, and d is the distance from the source. Clearly, if d is made equal to the focal length,

$$\Omega = \frac{\pi}{4f^2} \quad . \tag{11}$$

The total amount of radiation intercepted I_{in} can be determined from Equations 8 and 11:

$$I_{in} = \frac{h \, \nu_{nm} \, A_{nm} \, I_b \, Q_{\ell n} \, \ell_b \, \tau_n}{16 \, f^2 \, e} \quad . \tag{12}$$

Introducing a factor K to allow for the optical system losses in lenses, mirrors, and filters gives the intensity I_{PD} incident on a photodetector.

$$I_{PD} = \frac{K \, h \, \nu_{nm} \, A_{nm} \, I_b \, Q_{\ell n} \, N_\ell \, \ell_b \, \tau_n}{16 \, f^2 \, e} \quad . \tag{13}$$

In general, the emission intensity is a function of beam current

16

and gas density. The experiments of Schumacher and Gadamer (6) and Petrie (11) show that the intensity is linear with beam current and gas density up to at least one milliampere and a few hundred millitorr of pressure at room temperature in air. Therefore, within the above limitations the intensity can be considered linear with density.

Introducing the ideal gas law in the form shown by Kieffer and Dunn (14), parameters more easily measured experimentally are obtained.

$$I_{PD} = \frac{9.62 \times 10^{24} \; K \; h \; \nu_{nm} \; A_{nm} \; I_b \; Q_{\ell n} \; P \; \ell_b \; \tau_n}{16 \; f^2 \; e \; T} \; , \qquad (14)$$

where P is the pressure in Torr, T is the temperature in °K, and the other parameters are consistent with mks units.

The most inaccurate parameters in Equation 14 are the excitation cross-section $Q_{\ell n}$, the transition probability A_{nm}, and the lifetime of the excited state τ_n. The parameters A_{nm} and τ_n have been measured within an order of magnitude while $Q_{\ell n}$ may be more than an order of magnitude in error. Therefore, the accuracy of the calculation under the assumptions rests primarily on the accuracy of the excitation cross-section $Q_{\ell n}$.

A theoretical value for the excitation cross-section can be obtained by applying the Born approximation for inelastic excitation of molecules by fast electrons. For incident electron energies much in excess of the excitation threshold of the n level the collision cross-section for optically allowed excitation transitions to the n state from the ground state may be expressed by the following equation from Mott and Massey (15).

17

$$Q_{\ell n} = \frac{64\pi^5 m^2 e^4}{(2\pi m v/h)^2 h^4} \left| Z_{\ell n} \right|^2 \ell n \left\{ \frac{2mv^2}{E_n - E_\ell} \right\} .$$ (15)

Where $\left| Z_{\ell n} \right|$ is the matrix element of the transition, E_n is the energy of the excited state, E_ℓ is the energy of the ground state, v is the velocity of the incident electron, m is the mass of the electron, h is Plank's constant, and e is the electronic charge. From this expression it is clear that the cross-section for an optically allowed excitation transition varies as $E_e^{-1} \ell n E_e$, where E_e is the energy of the incident electron. The functional dependence of the excitation cross-section on electron energy shown in Equation 15 will be used later to estimate the cross-section for 10 Kev electrons from experimental data for low energy electrons.

II. INTENSITY RELATIONS IN HELIUM-AIR MIXTURES

It is necessary to consider specifically the radiation resulting from the interaction of the beam with helium and air. The energy level diagrams and prominent transitions for helium and nitrogen due to high energy electron beam excitation are given in Figure 4.

When a 10-50 KV electron beam passes through helium at densities below a few Torr and room temperature, the most prominent radiation is the atomic line at 5016 Å. This radiation results from excitation of the 1'S ground state of the helium atom to the 3'P excited state by the fast electrons and the subsequent spontaneous de-excitation of 5016 Å
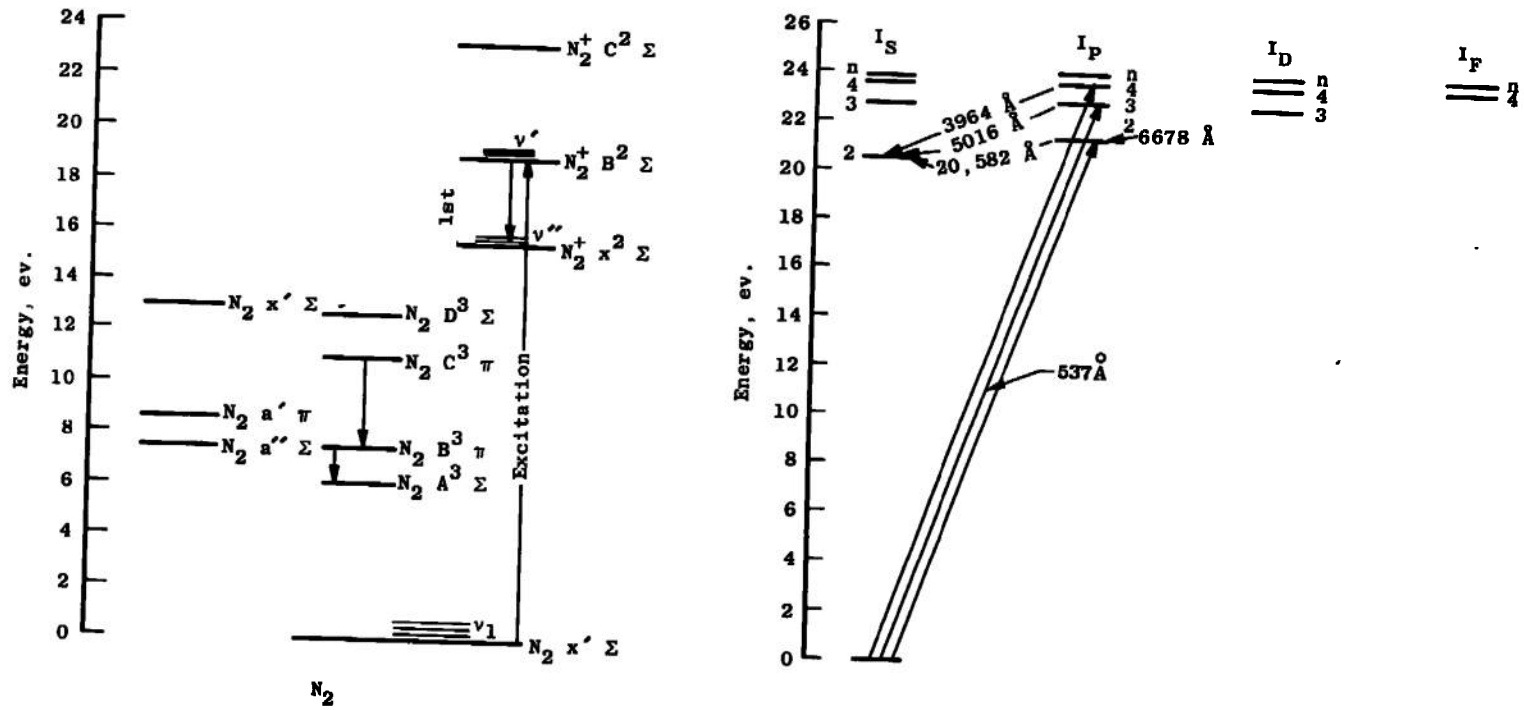
18

Fig. 4 Energy Level Diagram for Helium and Nitrogen

energy to the 2'S excited state. In the following discussion the parameters necessary for calculating the expected intensity of 5016 $\overset{\circ}{A}$ radiation will be obtained in the light of the assumptions made in deriving the equation for intensity of radiation from electron beam interaction with a gas.

First, consider the validity of assuming a single ground state. The ratio of the number of molecules in excited states to the number in the ground state is given by the Boltzman factor as shown by Herzberg (16).

$$\frac{N_n}{N_\ell} = \frac{g_n}{g_\ell} \; e^{-(E_n - E_\ell)/kT} \; , \tag{16}$$

where g_n and g_ℓ are the statistical weights of the upper and lower states, respectively, and the other parameters are as defined previously. For the 1'S ground state and 2'S excited state, which is the lowest excited state of helium, Equation 16 becomes,

$$\frac{N_n}{N_\ell} = e^{-\frac{2.35 \times 10^5}{T}} \; . \tag{17}$$

Equation 17 shows that for temperatures below 50,000°K, 99 per cent of the molecules are in the 1'S ground state. Also the probability of excitation, which is comparable to the transition probability in a relative sense, from excited states to the 3'P level is less than that from the 1'S ground state. Therefore, only one lower level need be considered and the single level assumption is valid.

In order to calculate the excitation cross-section for 10 KV

electrons, the value from Bauer and Bartky (17) for the excitation of
the 3'P level by 150 volt electrons, which is well above the excitation
level where the Born approximation and experimental values agree, will
be used in conjunction with the $E_e^{-1} \ln E_e$ electron energy dependence.

$$\frac{Q_{\ell n}}{Q_{150}} = \frac{E_e^{-1} \ln E_e}{E_{150}^{-1} \ln E_{150}} \quad . \tag{18}$$

The excitation cross-section for 10 KV electrons calculated from
Equation 18 is 0.82×10^{-23} m^2.

The population of the 3'P state is due to direct excitation since
transitions to higher states (from which cascading could occur) and
lower states (an intermediate step in two step excitation) are not
optically allowed. This can be easily deduced from the table of tran-
sition probabilities given by Wiese, Smith, and Glennon (18).

There are two major factors to consider for de-excitation of
the 3'P state. For a first order calculation collisional de-excitation
effects will not be considered. However, at high density this would
be a major contributor. The other factor is resonant excitation -
de-excitation of the 3'P state.

The 3'P excited level has a large cross-section for de-excitation
to the 1'S ground state emitting a 537 Å photon. This 537 Å photon is
quite readily absorbed by unexcited helium atoms, and can escape from
an enclosure only after many absorptions and re-emissions. Clearly
this phenomena will have an effect on the lifetime and the population
of the 3'P level of helium. As previously stated any diagnostic
technique of use in shock tunnels must have the capability of a

response time of a few tens of microseconds. It is necessary then to investigate the effect of resonance diffusion on the decay time of the 5016 Å helium line. The following analysis of the effect of resonance radiation on excited level lifetimes will follow the work of Holstein (19).

If N_0 atoms are excited to a reference level prior to t = 0, then the number remaining in this level as a function of time is determined by the equation,

$$N = N_0 \, e^{-qAt} \, , \tag{19}$$

where A is the probability per unit time for emission (the Einstein Coefficient) of a quantum of resonance radiation from an isolated atom, and q is the imprisonment factor. The imprisonment factor is less than unity and depends on the density, the shape of the containing vessel, and the dimensions of the containing vessel. The magnitude of q varies from zero to one. When the gas density is low q is equal to one and the lifetime of the 3'P level is determined entirely by spontaneous transition probabilities. At higher gas densities q goes to zero and the effect of resonance trapping is significant.

Heron, McWhorter, and Roderick (20), using pure helium, have shown that the lifetime of the 3'P level is determined largely by the phenomenon of imprisonment of resonance radiation, is pressure-dependent, and is of the same order of magnitude as the lifetimes measured for the 3914 Å and 4278 Å ionized nitrogen bands in a mixture of helium and nitrogen.

The Einstein Coefficient A is the reciprocal of the mean lifetime of the resonance level in the absence of imprisonment. The

imprisonment factor q, as given by Holstein (19) for a cylinder of infinite length with the radiation source at the centerline, is

$$q = \frac{1.60}{k_o R \ (\pi \ \ell n \ k_o R)^{1/2}} \ , \qquad (20)$$

where R is the radius of the containing vessel and, for a Doppler-broadened line, k_o is

$$k_o = \frac{\lambda^3 \ N}{8\pi} \ \frac{g2}{g1} \ \frac{1}{\tau_n \ V_o \ \pi^{1/2}} \ . \qquad (21)$$

Where

$$V_o = \sqrt{\frac{2kT}{m}} \ , \qquad (22)$$

is the most probable thermal speed of a helium atom, λ is the wavelength of the radiation, N is the number of unexcited helium atoms per cubic centimeter, k is Boltzman's constant, m is the molecular mass, and g_1 and g_2 are the statistical weights of the resonance and ground levels, respectively.

As previously stated any diagnostic technique of use in shock tunnels must have the capability of a response time of a few tens of microseconds. It is necessary then to investigate the effect of resonance diffusion on the decay time of the 5016 $\overset{o}{A}$ helium line.

In the case of the electron beam, the excited states are produced at a rate Q_o per unit time, the rate depending mainly on the electron current. The total excited in dt is $Q_o dt$. The intensity of the 5016 $\overset{o}{A}$ line can be expressed as a function of time as

$$I_{5016}(t) = h \, \nu_{5016} \, N_{3'P}(t) \, A_{3'P-2'S} \, . \tag{23}$$

The incremental number of atoms remaining in the resonant state due to the number of atoms excited in interval dt is

$$dN = Q_0 \, dt \, e^{-q'A't} = Q_0 \, e^{-q'A't} \, dt. \tag{24}$$

Integrating

$$N(t) = \int_0^n dN = \int_0^t Q_0 \, e^{-q'A't} \, dt, \tag{25}$$

$$N(t) = \frac{Q_0}{q'A'} \left(1 - e^{-q'A't}\right). \tag{26}$$

where q'A' is the sum of all transition probabilities and products of imprisonment factors and transition probabilities.

In the case of the 3'P state q'A' involves primarily the 5016 Å transition and the 537 Å transition, but only the 537 Å transition is resonant and has an imprisonment factor; therefore,

$$q'A' = q \, A_{537} + A_{5016} = \frac{1}{\tau_{3'P}} \, . \tag{27}$$

Thus,

$$N_{3'P}(t) = \frac{Q_0}{q \, A_{537} + A_{5016}} \left[1 - e^{-(qA_{537}+A_{5016})t}\right]. \tag{28}$$

Substituting Equation 28 into Equation 23,

$$I_{5016}(t) = h \, \nu_{5016} \, \frac{Q_0 \, A_{5016}}{q \, A_{537} + A_{5016}} \left[1 - e^{-(qA_{537}+A_{5016})t}\right]. \tag{29}$$

For example, assume the following representative values taken from Heron, McWhorter, and Roderick (20).

$$A_{5016} = 1.35 \times 10^7 \text{ sec}^{-1}, \tag{30}$$

$$A_{537} = 5.6 \times 10^8 \text{ sec}^{-1}, \tag{31}$$

$$\nu_{5016} = .99 \times 10^{15} \text{ Hertz}. \tag{32}$$

Substituting into Equation 29,

$$I_{5016}(t) = \frac{C}{56q + 1.35} \left[1 - e^{-(56q + 1.35) \times 10^7 t} \right]. \tag{33}$$

As pressure goes from zero to infinity, q goes from unity to zero. The extreme effect of resonance trapping occurs when the pressure approaches infinity. The decay time in this limiting case is the decay time of the 5016 Å transition which is 0.074 microseconds. Therefore, resonance diffusion will not preclude use of this line for data taken in observation times greater than one microsecond.

Finally, considerable survey spectra have shown the 5016 Å line sufficiently separated from other radiation in helium and air to be quite acceptable for diagnostic applications.

The above parameters and considerations compiled, the expected intensity according to Equation 14 may be calculated. Repeating for clarity,

$$\nu_{3'P-2'S} = c/\lambda_{3'P-2'S} = 5.96 \times 10^{14} \text{ sec}^{-1}, \tag{34}$$

where c is the speed of light,

$$A_{3'P-2'S} = 1.35 \times 10^7 \text{ sec}^{-1}, \tag{35}$$

$$Q_{1'S-3'P} = 0.82 \times 10^{-23} \text{ m}^2, \tag{36}$$

$$q = 1, \tag{37}$$

and

$$\tau_{n_{min}} = \frac{1}{A_{537} + A_{5016}} = 1.75 \times 10^{-9} \text{ sec.} \tag{38}$$

Substituting into Equation 14,

$$I_{He} = 1.15 \times 10^{-10} \frac{9.62 \times 10^{24} K_{He} h I_b P \ell_b}{16 f^2 e T} \text{ watts.} \tag{39}$$

where P is in Torr, T is in °K, K_{He} is the transmission factor for the optical system, and the other parameters are consistent with mks units.

In a similar manner the interaction of an electron beam with air will be discussed. In air, under conditions comparable to those considered for helium, the most prominent radiation is due to what is called the first negative system of ionized nitrogen. This system consists of several vibrational bands with the strongest band having its bandhead at 3914 Å. This system results from excitation of the $N_2 X' \Sigma$ ground electronic state of the stable nitrogen molecule to the $N_2^+ B^2 \Sigma$ excited state of the singly ionized nitrogen molecule by the fast electrons and subsequent spontaneous de-excitation, which results in the first negative system, to the $N_2^+ X^2 \Sigma$ state of the ionized molecule. The nitrogen system is inherently much more complicated than atomic helium since each vibrational band is approximately forty Å

wide and consists of a number of rotational lines [see Muntz (7)]. However, by considering each vibrational band to be a single line, as it would appear on a spectrograph with poor resolution, an analysis similar to the analysis of helium may be carried through.

Consider the validity of assuming a single ground vibrational state. The ratio of the number of molecules in the first excited vibrational state of the neutral molecule to the number in the ground state is given by Herzberg (8) as 1.4×10^{-5} at 300°K and 0.035 at 1000°K. At a temperature of 1000°K, 96.5 per cent of the molecules are in the ground vibrational state. This requirement is not critical since the excitation cross-section used for subsequent calculations is the total cross-section for the excitation of the 4278 Å vibrational band.

A rigorous calculation of the excitation cross-section using the Born approximation has been done by Hornkohl (21). These calculations have been done for the purpose of studying high energy electron excitation and have shown good functional agreement with experimental data by Sheridan (22). These data will be used for nitrogen excitation cross-section.

A considerable amount of investigation on the excitation-emission path in nitrogen has been done by several authors. Muntz (7) gives an exhaustive discussion with the conclusion that the excitation to the N_2^+ $B^2\Sigma$ state is a direct excitation and it may be considered the only path of excitation. Measurements of the mean lifetime by Bennet and Dalby (23) have shown that it is not affected by

density up to at least 1.5×10^{16} atoms per cm^3 (470 millitorr at room temperature). Therefore, this system should be satisfactory for air diagnostics and the model assumed previously should be acceptable for first order absolute intensity calculations. Finally, as was done with helium, considerable search spectra were taken to determine what portion of the system should be used. Although the 3914 Å band is the strongest the 4278 Å band was chosen because early experiments demonstrated a noticeable interference from the 3889 Å atomic line in helium.

The above parameters and considerations compiled, the expected intensity according to Equation 14 may be calculated for the 4278 Å (0,1) band of nitrogen. The parameters are,

$$\nu_{N_2^+B^2\Sigma - N_2^+X^2\Sigma}(0,1) = c/4278 \text{ Å} = 7.0 \times 10^{14} \text{ sec}^{-1}, \quad (40)$$

$$A_{N_2^+B^2\Sigma - N_2^+X^2\Sigma}(0,1) = 0.220 \times 10^7 \text{ sec}^{-1}, \quad (41)$$

$$Q_{N_2X'\Sigma - N_2^+B^2\Sigma} = 0.149 \times 10^{-22} \text{ m}^2, \quad (42)$$

and

$$\tau_{N_2^+B^2\Sigma}(0,1) = 6.58 \times 10^{-8} \text{ sec}. \quad (43)$$

Substituting into Equation 14,

$$I_{N_2} = 1.51 \times 10^{-9} \frac{9.62 \times 10^{24} K_{N_2} h I_b P_{N_2} \ell_b}{16 f^2 e T} \text{ watts}. \quad (44)$$

Where P is in Torr, T is in °K, K_{N_2} is the transmission factor for the optical system, and the other parameters are in mks units.

In order to get a more positive indication of the arrival of a

given percentage of helium, say ten per cent, at the test section where the flow density is often changing quite rapidly, the ratio of helium intensity to air intensity was measured directly. Density has a compound effect on intensity because intensity is directly dependent on density and beam current while beam current is dependent on density due to beam attenuation. The constants K_{He} and K_{N_2} in Equations 39 and 44 are the constants for a particular channel as shown in Figure 2, page 8.

According to Dalton's law of partial pressures, each gas in a mixture of gases exerts pressure in proportional part by volume. Therefore, in a volume percentage mixture of helium and nitrogen the pressure in Equations 39 and 44 become the partial pressures of helium and nitrogen. Taking the ratio of Equation 30 to Equation 44,

$$\frac{I_{He}}{I_{N_2}} = \frac{1.15 \times 10^{-10} \, K_{He} \, P_{He}}{1.51 \times 10^{-9} \, K_{N_2} \, P_{N_2}} \quad , \tag{45}$$

The parameters of beam current, beam area, length of beam observed, temperature, and system f number do not appear in Equation 45. Equation 45 may be written in terms of a volume percentage:

$$\frac{I_{He}}{I_{N_2}} = 0.076 \, \frac{K_{He} \, (\%He)}{K_{N_2} \, (\%N_2)} \quad . \tag{46}$$

Since nitrogen is seventy-eight per cent by volume of air, Equation 46 may be written for air:

$$\frac{I_{He}}{I_A} = 0.098 \, \frac{K_{He} \, (\%He)}{K_A \, (\% A)} \quad . \tag{47}$$

The constant K_{He}/K_A is a characteristic of the electro-optical system and may be determined using a standard intensity source. In practice, it has proven convenient to plot the intensity ratio versus the percentage ratio giving a linear plot with slope 0.098 K_{He}/K_A. In this manner the system calibration curve may be obtained from a single calibration point.

As a cursory check on Equation 46 the data of Sebacher [13] were considered. These data consist of spectra taken in static mixtures of helium and air excited by a high energy electron beam. Assuming the data are corrected for system constants, which appear to be the case since the ratio of N_2^+ (0,0) intensity to N_2^+(0,1) intensity is 3.5 compared to a theoretical value of 3.35, the ratio of 5016 Å helium intensity to 4278 Å nitrogen peak intensity is 0.96 for a mixture of 87 per cent helium and 13 per cent nitrogen. From Equation 46 a ratio of 0.51 is calculated for the same mixture and a K_{He}/K_A of unity. This agreement is reasonable considering the order of magnitude accuracy of some parameters in the analysis.

CHAPTER IV
MEASUREMENTS OF PERCENTAGE CONCENTRATION IN HELIUM-AIR MIXTURES

I. RELATIVE INTENSITY MEASUREMENT

As the previous analysis has shown, there is a considerable advantage in obtaining the ratio of intensities when measuring volume percentages in a mixture of helium and air. This could be done by utilizing the individual photomultiplier outputs for helium and air intensity. However, as is the usual case for shock tunnel data, this information is recorded on oscilloscopes which makes point by point data reduction inaccurate. Also, as is shown in Figure 5, due to the dependence of absolute intensity on several variables the individual oscilloscope traces are quite irregular. This fact contributes additional error to ratio data obtained from the individual oscillo-scope traces. Therefore, it was necessary to obtain the "in line" ratio as the data were generated during a shock tunnel run.

The Donner Model 3732 diode quarter-square multiplier used to take the "in line" intensity ratio is shown in block diagram form in Figure 6, page 33. The heart of this operation is a diode and resistor network with an output proportional to the square of the in-put. By proper selection of resistors in a parallel combination of several sets of one resistor and a diode in series this squaring function can be closely approximated in a "piecewise linear" fashion.
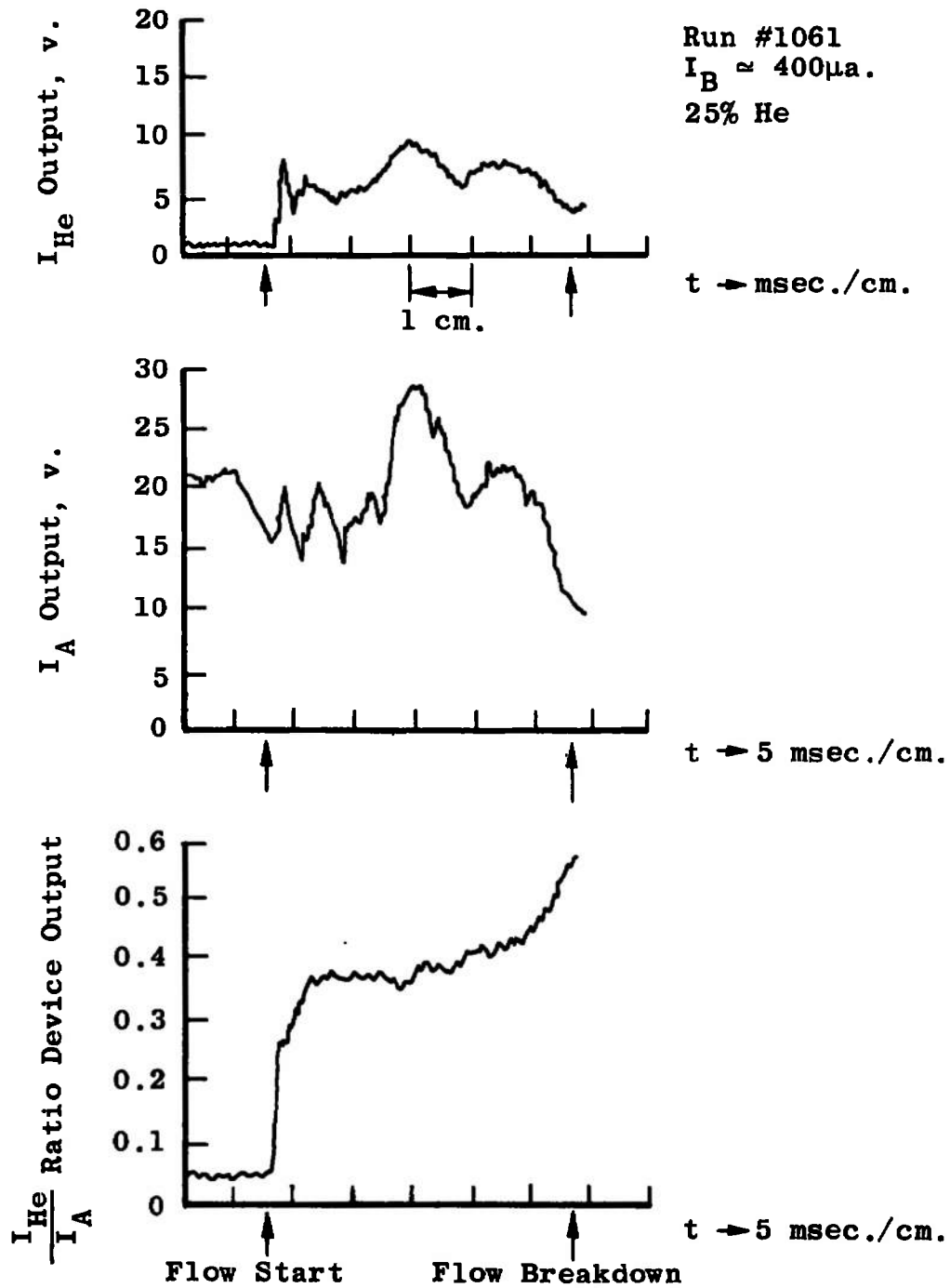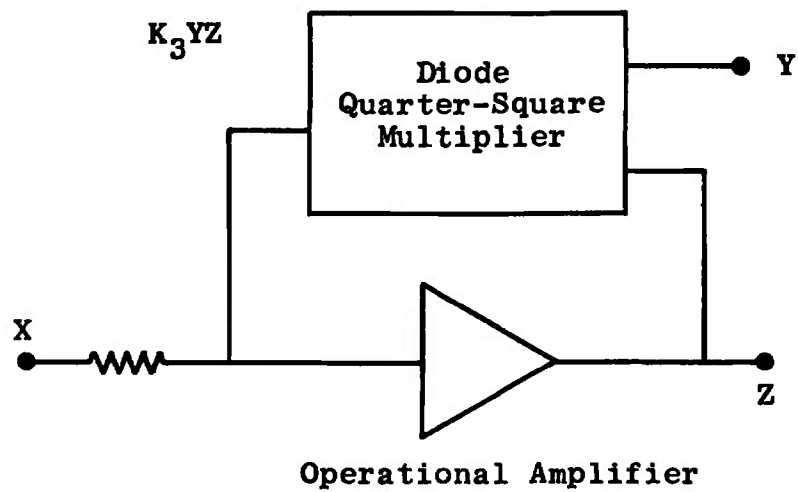
Fig. 5 Comparison of Raw Data to Ratio Device Output

$$K_3 YZ$$

Diode
Quarter-Square
Multiplier

Y

X

Z

Operational Amplifier

$$Z = -\frac{X}{K_3 Y}$$

Fig. 6 Block Diagram of Ratio Device

Two of these squaring circuits can then be combined to solve

$$K_1 \left(\frac{Z+Y}{2}\right)^2 - K_2 \left(\frac{Z-Y}{2}\right)^2 = K_3 ZY. \qquad (48)$$

Assuming Z in Figure 6 to be the output of the operational amplifier, the multiplier output, according to Equation 48, is $K_3 YZ$. Summing the inputs to the operational amplifier, realizing the amplifier draws negligible current, gives

$$X = - K_3 YZ. \qquad (49)$$

Therefore,

$$Z = - \frac{X}{K_3 Y} \cdot \qquad (50)$$

If the helium photomultiplier output is made the X input and the air photomultiplier output is made the Y input the intensity ratio is obtained directly.

A comparison of the individual photomultiplier outputs and the ratio output from the divider is shown in Figure 5, page 32. The advantage of this technique is evident. Despite the irregularity of the individual helium and air intensities the ratio was readily obtained. All of the dynamic data were obtained using the ratio device.

II. RELATIVE INTENSITY MEASUREMENTS IN A STATIC GAS

In order to assess system quality and determine static calibration constants a static evaluation was performed. A small static test section was placed over the electron gun exit orifice. The beam

was viewed by the optics through a plexiglass port. In this manner the system was calibrated in the same physical configuration in which it was used to make later dynamic tests. Mixtures of helium and air from high pressure bottles were leaked into the test section and the ratio of helium channel output to air channel output was taken. This method of obtaining mixtures was found to be much more consistent than any form of low pressure mixing. The static calibration data are plotted in Figure 7. Since the primary interest was in detecting the arrival of a ten per cent concentration of helium extensive calibration was only done up to mixtures of twenty-five per cent. This range is most accurate for relative measurements because accurate high helium percentages are not as easily obtained. Leaks in the vacuum system are more negligible at high percentages of air.

Before the data in Figure 7 can be compared with the theoretical result in Equation 47 it is necessary to look more closely at the transmission of the optical system. A composite of the optical system components with variable transmission versus wavelength is shown in Figure 8, page 37. From Figure 8, it is observed that the constant K_{He}/K_A is determined in the following manner:

$$\left(\frac{I_{He}}{I_A}\right)_{SL} = \frac{K_{He} \int S(\lambda)\ F_{He}(\lambda)\ d\lambda}{K_A \int S(\lambda)\ F_A(\lambda)\ d\lambda} \ . \tag{51}$$

Where $S(\lambda)$ is the standard lamp output function and $F_{He}(\lambda)$ and $F_A(\lambda)$ are the filter transmission functions. An estimate of K_{He}/K_A is obtained by simply considering the standard lamp intensity at the
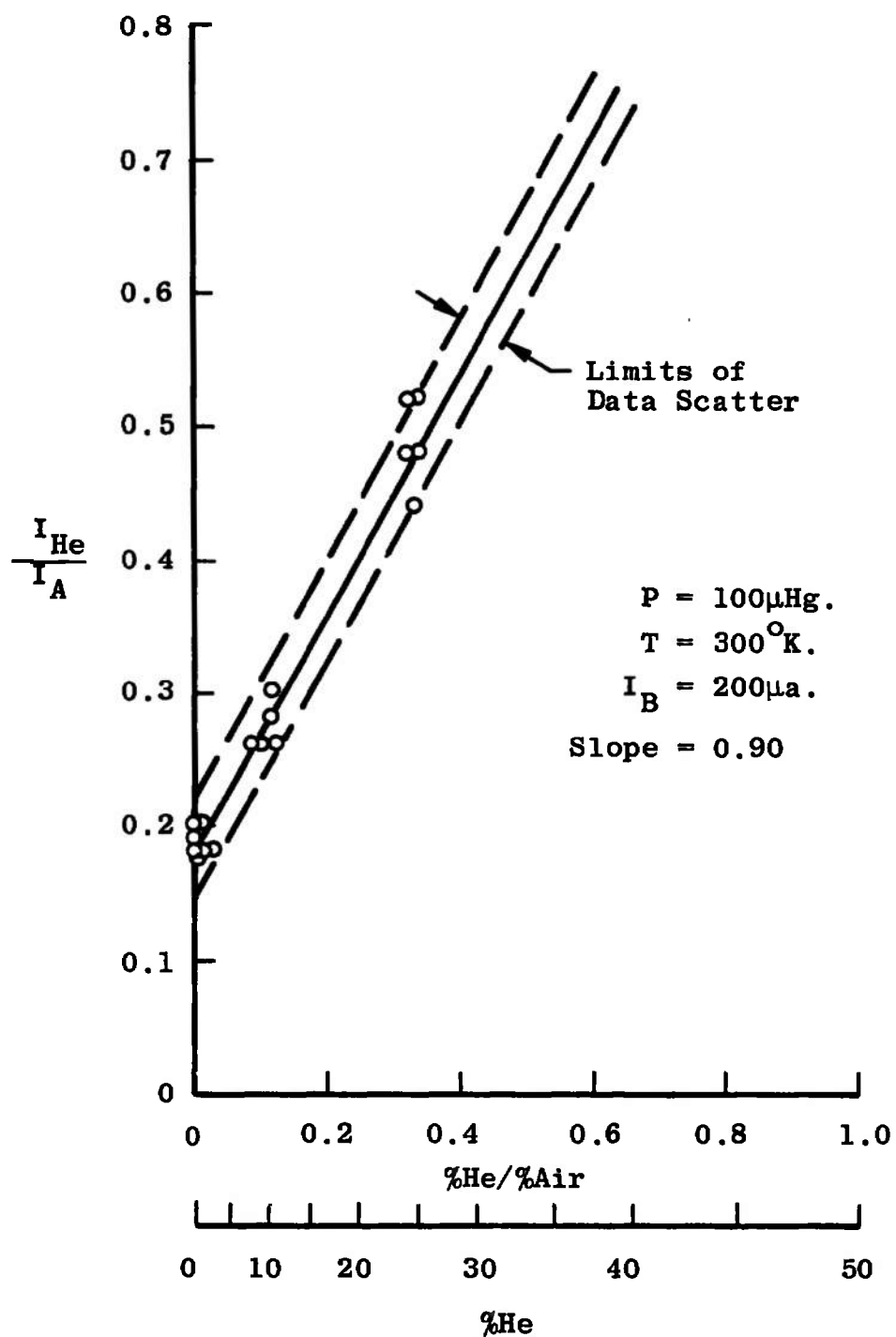
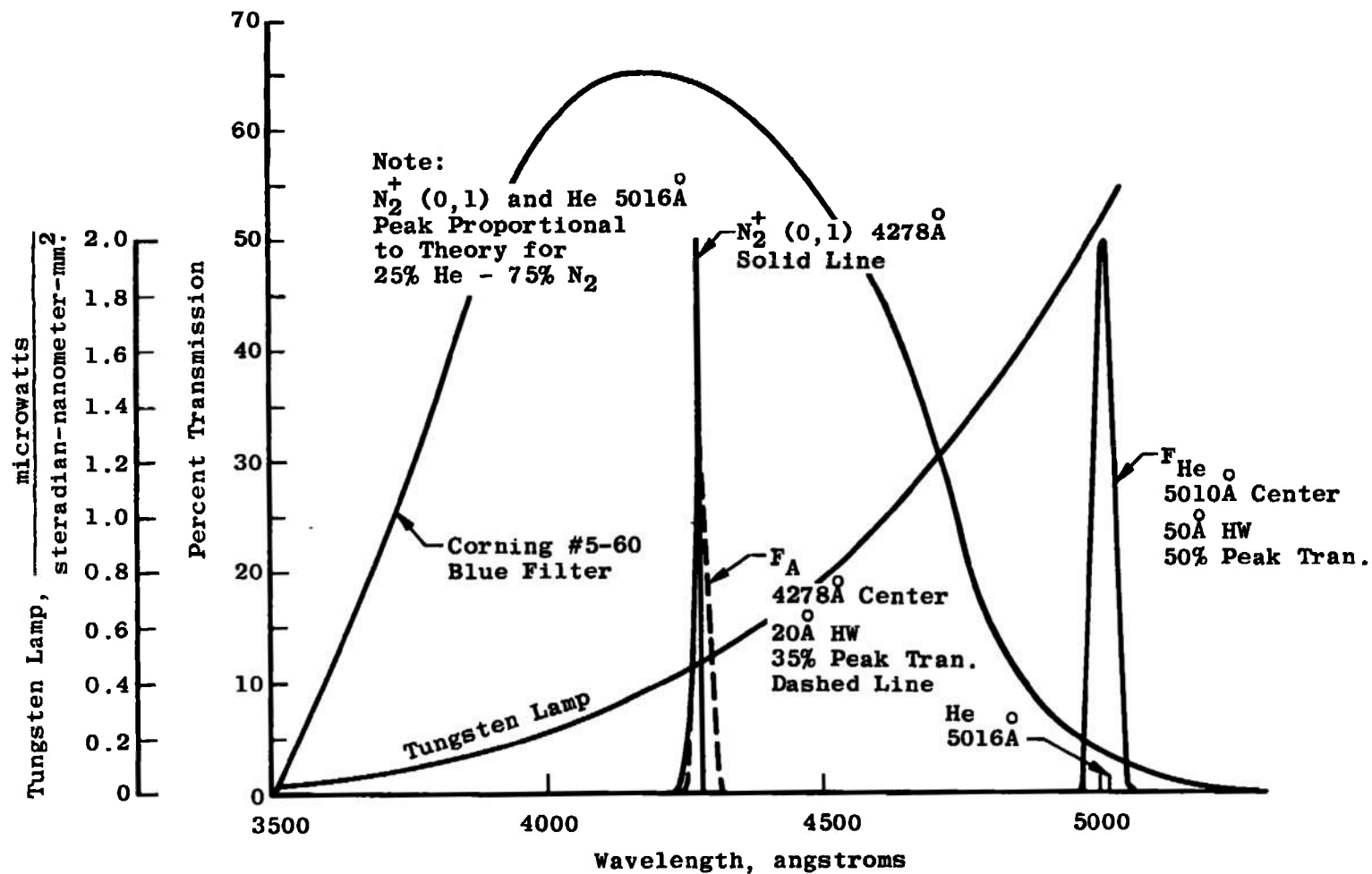Fig. 7 Interface Detection System Static Calibration

Fig. 8 Composite of Optical Component Transmission

filter transmission peak, the relative peak transmission of the filters, and the relative half width of the filters. Using these approximations in Equation 51,

$$\left(\frac{I_{He}}{I_A}\right)_{SL} = \frac{K_{He}}{K_A} \frac{S_{5016}}{S_{4278}} \frac{F_{He(peak)}}{F_{A\,(peak)}} \frac{F_{He\,(HW)}}{F_{A\,(HW)}} \frac{F_{blue(5016)}}{F_{blue(4278)}} .$$

Substituting values from Figure 8,

$$\left(\frac{I_{He}}{I_A}\right)_{SL} = \frac{K_{He}}{K_A} \frac{2.06 \times 50 \times 50 \times 3}{0.47 \times 35 \times 20 \times 65} . \tag{52}$$

The measured ratio of I_{He} to I_A for the standard lamp was 1.2. Substituting this value into Equation 52 gives

$$\frac{K_{He}}{K_A} = 1.7. \tag{53}$$

This interface detection system was designed to measure per cent concentration of helium. Interpretation of data with regard to absolute determination of excitation cross-sections or other parameters is not reasonable. However, it should compare on an order of magnitude basis with relative measurements of helium and nitrogen parameters. Using the approximation that the nitrogen filter has uniform response throughout the N_2^+ (0,1) band, it is quite easy to compare the prediction of Equation 47 with the results shown in Figure 7, page 36. Substituting the value for K_{He}/K_A from Equation 53 into Equation 47 gives

$$\frac{I_{He}}{I_A} = 0.17 \frac{\%\ He}{\%\ Air} . \tag{54}$$

From Figure 7, page 36, it is seen that

$$\frac{I_{He}}{I_A} = 0.90 \frac{\%\ He}{\%\ Air} . \tag{55}$$

There are two primary sources of error which contribute to the

inequality of Equations 54 and 55. As has been stated the error in the theoretical parameters may easily total an order of magnitude. In addition, the errors in data acquisition contribute directly to the values in Equation 55.

III. RELATING INTENSITY MEASUREMENTS IN A TRANSIENT GAS MIXTURE OF HELIUM AND AIR

The ultimate purpose of the interface detection system is to measure the time-resolved percentage of helium in a helium-air mixture which is transient with respect to space and time. Data were taken at a single point in the shock tunnel test section.

Two experiments were undertaken to determine the validity of the system. First, the driven tube was charged with zero, ten, and twenty-five per cent volume mixtures of helium and air. Operation of the shock tunnel shown in Figure 1, page 2, as near its optimum condition as possible with varying mixtures in the driven tube gave a known gas mixture in the test section for from ten to twenty milliseconds. Actual traces of the ratio device output are shown in Figure 9. The maximum apparent step response of two milliseconds indicates that there are no transient effects of resonance diffusion or collisions which invalidate the data shown in Figure 9 which is essentially constant for ten to twenty milliseconds. Complete results of the dynamic evaluation are plotted in Figure 10, page 41. Each data point represents a tunnel run. From this curve the following dynamic equation is derived,
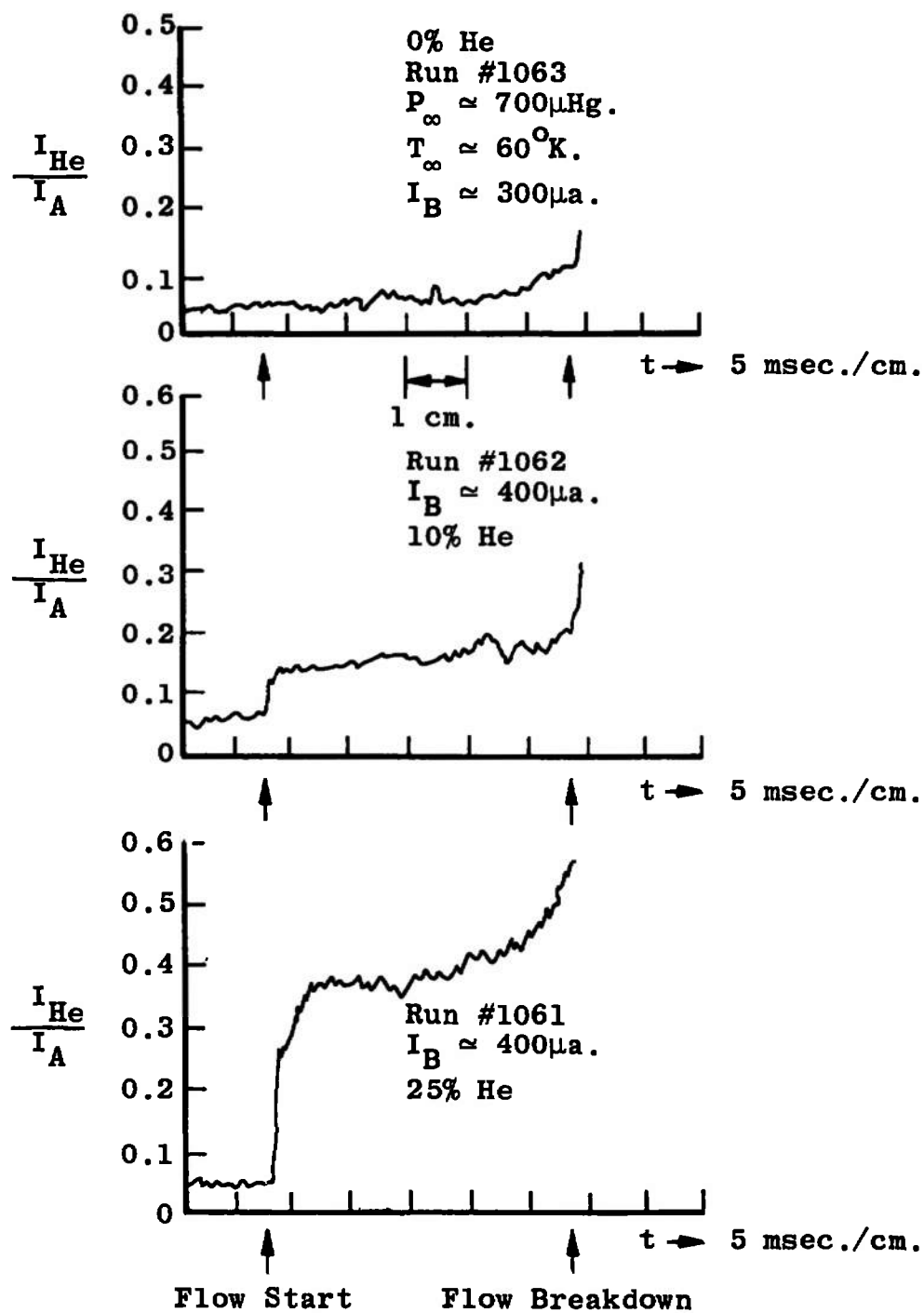
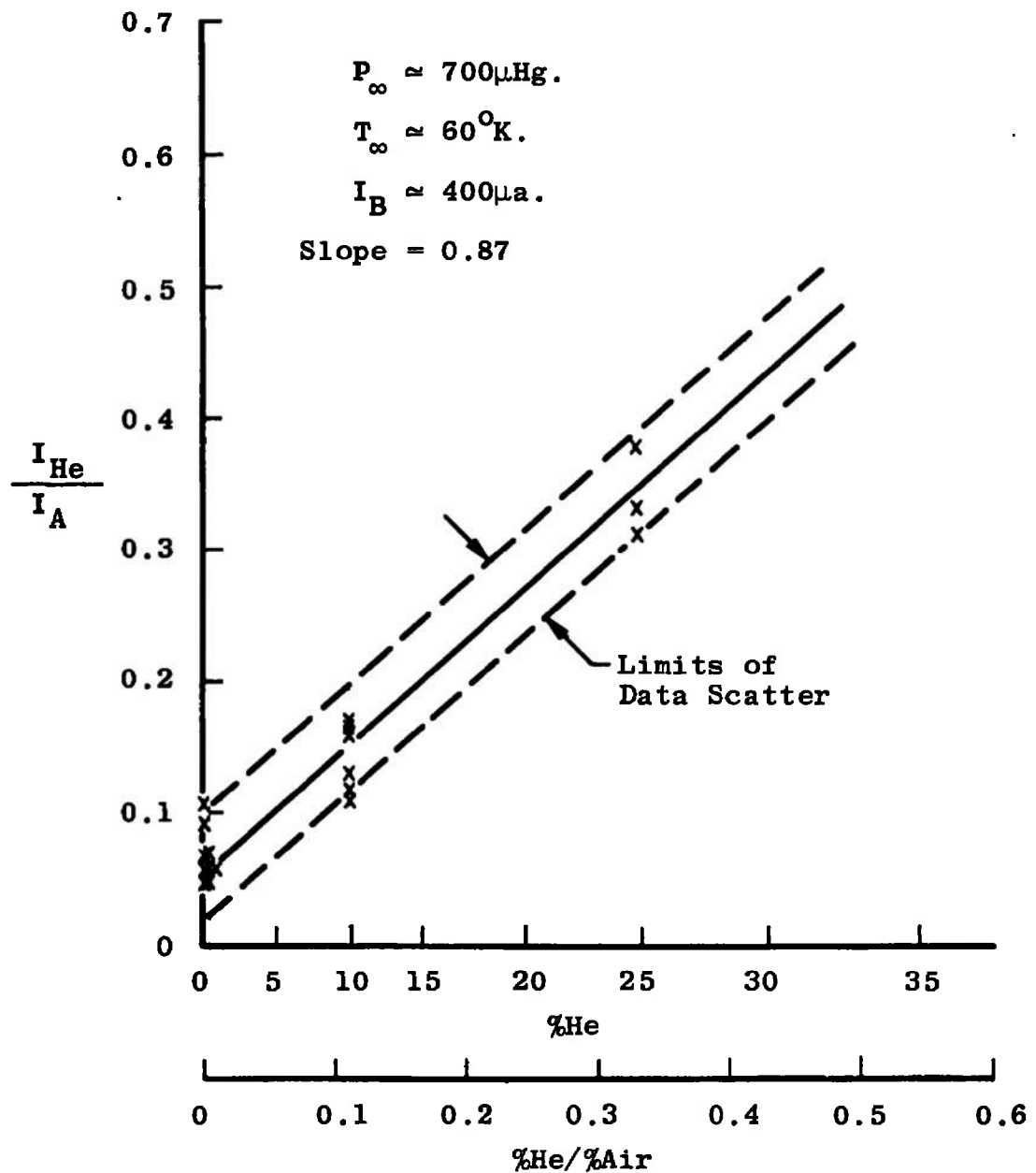Fig. 9 Oscilloscope Traces of Intensity Ratio Versus Time

Fig. 10 Interface Detection System Dynamic Evaluation

$$\frac{I_{He}}{I_A} = 0.87 \frac{\% \ He}{\% \ Air} \ . \tag{56}$$

In the second experiment a buffer section and diaphragm were added so that the arrival time of the helium interface could be varied in a predictable manner. The results of this experiment are shown in Figure 11. A diagram of the shock tunnel configuration is also shown in Figure 11. It is clear that as the interface diaphragm location was moved closer to the test section, the helium arrived at the test section earlier.

The linear relationship between the ratio of helium percentage. to air percentage of the transient gas and the ratio of helium intensity to air intensity shown in Figure 10 indicates that the interface detection system is indeed measuring the per cent concentration of helium and air. At a helium concentration of ten per cent the scatter of the data in Figure 10 indicates an accuracy of ±4 per cent in the measurement of helium concentration. The data in Figure 11 show the ability of the system to detect the arrival of a helium-air interface.

During early evaluation of the system the radiation detected by the helium channel during a tunnel run with no electron beam present was investigated. At this point in the development the helium channel contained a filter with a 200 $\overset{o}{A}$ half width. It was found that on some runs the helium channel exhibited enough background radiation to cause questionable results for low percentages of helium. The background radiation was not significantly greater than the emission level resulting from low percentages (< 10 per cent) of helium. A helium filter
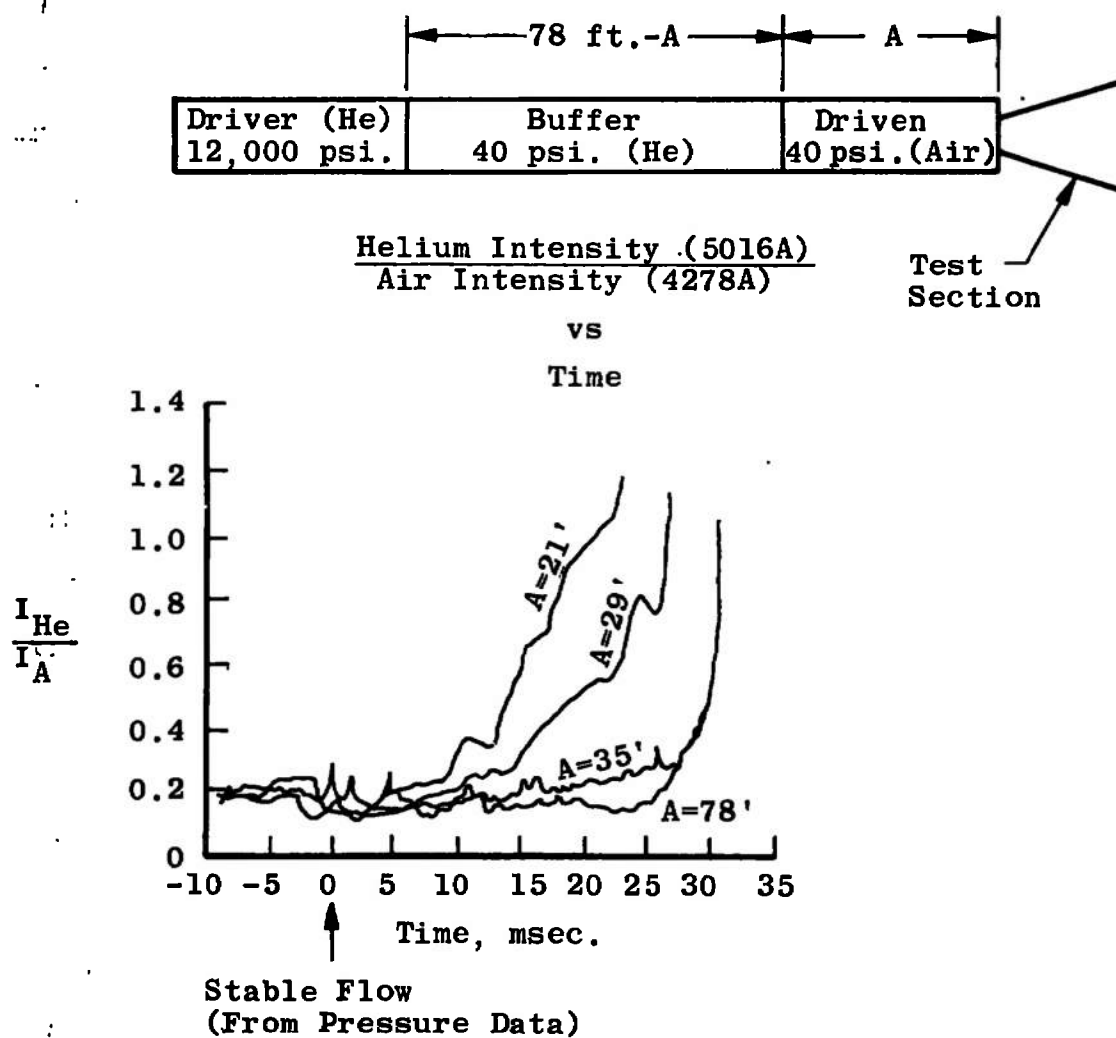
Fig. 11 Buffer Gas-Driven Gas Interface Arrival Time Study

with 50 Å half width was placed in the helium channel which reduced the background radiation to an acceptable level. The data in Figure 11 were taken with the 200 Å filter. This is the reason for the difference in intensity ratio for air in the early part of the trace. This also shows the need for careful consideration of background radiation in such systems.

Another result of system imperfection which is evident in both Figure 7, page 36, and Figure 10, page 41, is that a zero helium per cent does not give an intensity ratio of zero. The primary reason for this is that the helium channel indicates some output due to the much stronger nitrogen emission. Also the imperfect null of zero frequency components in the output circuits is another contributor.

CHAPTER V
CONCLUSIONS

An electron beam excitation system and a specialized spectrometer for measuring transient gas concentrations in a shock tunnel have been developed. Evaluation data demonstrated that the system is capable of detecting the percentage of helium in a transient helium air mixture within ±4 per cent of helium percentage. There did not appear to be any degrading effects due to variations in beam current (0-1 ma), pressure (0.05-1 Torr), or temperature (60-300°K). Also, the time response of the device to changes in mixture concentration indicates that there are no transient effects due to resonance diffusion in helium or collision effects between molecules of the same gas or molecules of different gases in a helium-air mixture which would invalidate transient concentration measurements taken on a time scale of a few milliseconds.

There are at least five areas which warrant further study if the ultimate potential of gas concentration measurements with the electron beam is to be realized:

1. The effects on electron beam emission of densities equivalent to several Torr at room temperature need further work. There are many cases where density and gas concentrations could be of value if a firm upper limit for density were established.

2. In conjunction with high density studies much could be

45

learned about the resonance diffusion and collision effects mentioned above since they will be the limiting conditions on higher density work.

3. It is evident from the theoretical calculations of electron beam excited emission that the present values for excitation cross-section and even lifetimes will have to be improved if theoretical designs of such systems are to be done with confidence.

4. A need which is too often put aside is the need for a high current (10 ma), high voltage (50-100 KV) electron gun which is easily adapted to experimental apparatus. High quality gun operation is prerequisite to any viable data acquisition.

5. Additional capabilities in the instrumentation system would be advantageous. With proper interpretation of the effects of beam spreading, beam attenuation, and catcher cup current measurements, additional dividers could be added to take the ratio of absolute intensity and beam current, thereby obtaining the density of helium and air directly. Also, a beam modulation and detection system, which is discussed in the Appendix, would reduce the effect of background radiation.

BIBLIOGRAPHY

1. Hertzberg, A., and others. "Modifications of the Shock Tube for the Generation of Hypersonic Flow," Arnold Engineering Development Center TN-55-15, Arnold Air Force Station, Tennessee, 1955.

2. Kaegi, E. M. and E. P. Muntz. "Driver-Driven Gas Mixing and Its Effect on Shock Tunnel Test Time," Third Hypervelocity Techniques Symposium, Denver, Colorado, March, 1964.

3. Muntz, E. P. and D. J. Marsden. Rarefied Gas Dynamics II. Edited by J. A. Laurmann. New York: Academic Press, 1963.

4. Copper, J. A., H. R. Miller, and F. J. Hameetman. "Correlation of Uncontaminated Test Durations in Shock Tunnels," Fourth Hypervelocity Techniques Symposium, Arnold Air Force Station, Tennessee, November, 1965.

5. Bird, K. D., J. F. Martin, and T. J. Bell. "Recent Developments in the Use of the Hypersonic Shock Tunnel as a Research and Development Facility," Third Hypervelocity Techniques Symposium, Denver, Colorado, March 1964.

6. Schumaker, B. W. and E. O. Gadamer. "Electron Beam Fluoresence Probe for Measuring the Local Gas Density in a Wide Field of Observation," Canadian Journal of Physics, 36: 659-671, 1958.

7. Muntz, E. P. "Measurement of Rotational Temperature, Vibrational Temperature, and Molecule Concentration in Non-Radiating Flows of Low Density Nitrogen," University of Toronto Institute of Aerophysics Report 71, Toronto, Canada, April, 1961.

8. Herzberg, G. Spectra of Diatomic Molecules. Princeton, New Jersey: Van Nostrand Company, Inc., 1950.

9. Muntz, E. P. "Direct Measurement of Velocity Distribution Functions," Proceedings of the Fourth International Symposium on Rarefied Gas Dynamics, Toronto, Canada, July, 1964.

10. Muntz, E. P., S. J. Abel, and B. L. Maguire. "The Electron Beam Fluorescence Probe in Experimental Gas Dynamics," Institute of Electrical and Electronic Engineers Conference on Aerospace, Houston, Texas, June, 1965.

11. Petrie, S. J. "An Electron Beam Device for Real Gas Flow Diagnostics," Aerospace Research Laboratories Report 65-122, Columbus, Ohio, June, 1965.

12. Froedge, D. T. "High Energy Electron Beam Excitation of a Gas," Unpublished Masters thesis, The University of Tennessee Space Institute, Tullahoma, Tennessee, 1967.

13. Sebacher, D. I. "Study of Collision Effects Between the Constituents of a Mixture of Helium and Nitrogen Gases when Excited by a 10 KV Electron Beam," Journal of Chemistry and Physics, 42:1358-1372, February, 1965.

14. Kieffer, L. J. and G. H. Dunn. "Electron Impact Ionization Cross-Section Data for Atoms, Atomic Ions, and Diatomic Molecules: I Experimental Data," Reviews of Modern Physics, 38:3, January, 1966.

15. Mott, N. F. and H. S. W. Massey. The Theory of Atomic Collisions. London: Oxford University Press, 1952.

16. Herzberg, G. Atomic Spectra and Atomic Structure. New York: Dover Publications, 1944.

17. Bauer, E. and C. D. Bartky. "Calculation of Inelastic Electron-Molecule Collision Cross Sections by Classical Methods," Journal of Chemical Physics, 43:2469, October, 1965.

18. Wiese, W. L., M. W. Smith, and B. M. Glennon. Atomic Transition Probabilities - Hydrogen Through Neon. National Bureau of Standards, United States Department of Commerce, NSRDS-NBS4, Vol. I. Washington: Government Printing Office, 1966.

19. Holstein, T. "Imprisonment of Resonance Radiation in Gases II," Physical Review, 83:1159-1168, September, 1951.

20. Heron, S., R. W. P. McWhorter, and E. H. Roderick. "Measurements of Lifetimes of Excited States of the Helium Atom," Proceedings of the Royal Society of London, 234A:565-582, March, 1956.

21. Hornkohl, J. O. Private Communication. ARO, Inc., Arnold Air Force Station, Tennessee, October, 1967.

22. Sheridan, W. F. Private Communication. Air Force Cambridge Research Laboratory, Bedford, Massachusetts, April, 1967.

23. Bennet, R. G. and F. W. Dalby. "Experimental Determination of the Oscillator Strengths of the First Negative Bands of N_2^+," The Journal of Chemical Physics, 31:434-441, August, 1959.

24. Arecchi, F. T., E. Gatti, and A. Sona. "Measurement of Low Light Intensities by Synchronous Single Photon Counting," The Review of Scientific Instruments, 37:942-948, July, 1966.

25. Schwartz, L. P. Principles of Coding, Filtering, and Information Theory. Baltimore: Spartan Books Incorporated, 1963.

.

APPENDIX

.

APPENDIX
SIGNAL TO NOISE IMPROVEMENT IN EXTERNALLY EXCITED,
MILLISECOND DURATION, RADIATION PHENOMENA

A significant improvement in accuracy could be obtained by eliminating the effects of background radiation from the electron beam excited radiation. A study of possible methods was made following the work discussed as the subject of this thesis.

There are several approaches which have been used successfully to improve the signal to noise ratio of spectroscopic data taken on a one second or greater time scale. Quite often narrow band optical and electrical filters are sufficient. However, in electron beam diagnostics in shock tunnel flows a significant background level passes through even a narrow optical filter and the electrical filter must have a bandwidth sufficient to satisfy millisecond response requirements.

In cases where the noise is sufficiently random and the photon arrival rate is low enough, single photon counting techniques have been utilized by Arecchi, Gatti, and Sona (24). However, they state that for counting systems with microsecond response the necessity of no appreciable counting losses limits single photon counting techniques to photoelectron arrival rates less than 10^5 photoelectrons per second. Assuming that system response is not a limiting factor it is revealing to consider the number of photons necessary to establish a valid average data point every 100 microseconds. Assuming the arrival rate of

photoelectrons at the anode has a Poisson distribution the error in
determining the average number of counts for a fixed sampling period is,

$$\sigma = \sqrt{N}. \tag{57}$$

Where σ is the standard deviation of the number counted per sampling
period and N is the average number counted per sampling period. In
order to obtain a standard deviation which is ten per cent of the aver-
age number counted per sampling period, a total of 10^2 photoelectrons
must be counted per sampling period. For a typical photocathode quan-
tum efficiency of ten per cent this means 10^3 photons must be incident
on the photocathode per sample period. If the sample period is taken
as 100 microseconds then the required photon arrival rate is 10^7
photons per second. The photon arrival rates inherent in the data
acquired in this work were on the order of 10^7 photons per second.
However, while the information rate is sufficient the unavailability
of submicrosecond counting equipment precluded immediate investigation
of this technique.

Lock-in or synchronous amplification, where the excitation
source is modulated and the output is phase detected, has been used
quite successfully. The operation of synchronous detection is related
quite succinctly by Schwartz (25).

"The message function $f_m(t)$ is modulated into a cosine carrier
at the transmitter to give

$$f_s(t) = f_m(t) \cos w_o t. \tag{58}$$

At the receiver the incoming signal is multiplied by a cosine reference voltage of the same frequency and phase as the carrier. The result is

$$f_m(t) \cos^2 w_o t = \frac{f_m(t)}{2} (1 + \cos 2w_o t). \tag{59}$$

The signal is then passed through a low-pass filter which eliminates the double carrier frequency term. The output is $1/2 \; f_m(t)$."

By making the low-pass filter narrow band about zero frequency the signal to noise ratio can be greatly enhanced.

In applications of interest here where the output bandwidth cannot be made arbitrarily narrow the remaining advantages are the 3 db increase in signal to noise ratio, as indicated by Schwartz (25), and the shifting of information to higher frequencies where the noise should be reduced if it follows the common 1/f energy spectrum. Schwartz (25) also indicates that the greatest advantage to synchronous detection is for signal to noise ratios less than one.

In most transient cases presently of interest the signal to noise ratio is greater than one. Also, a brief experiment with a Lock-In amplifier showed that the phase shift through the electron beam excitation system is not constant. Therefore, it was deemed prudent to investigate a less complicated amplitude modulation and detection scheme which should give considerable improvement in signal to noise ratio since it incorporates the primary advantage of synchronous detection by shifting information to higher frequencies.

A block diagram of the signal extraction system is shown in
Figure 12. For convenience a 455 kilohertz modulation frequency was
selected because conventional intermediate frequency components are
available. The modulation signal was capacitance coupled into the con-
trol grid of the electron gun through a 455 kilohertz intermediate
frequency transformer. A second 455 kilohertz output transformer was
used at the output to tune the photomultiplier output circuit to the
carrier frequency. Noise was introduced by modulating a neon bulb
biased in the glow regime by a battery. A diode detector was used to
provide a dc signal at the output.

There are two points which warrant comment regarding this
technique. It is imperative that the beam be modulated cleanly. Any
amplitude variation of the carrier at the input will be transmitted
through to the output. It is of interest to note that when a diode is
used as a detector and the carrier is greater in magnitude than the
noise frequencies near the carrier frequency, the carrier switches the
diode and therefore tends to enhance only information in phase with the
carrier. For this condition amplitude detection is somewhat analogous
to synchronous detection.

Using the system shown in Figure 12, signal to noise improvement
of 10^3 was readily obtained. A plot of signal to noise improvement
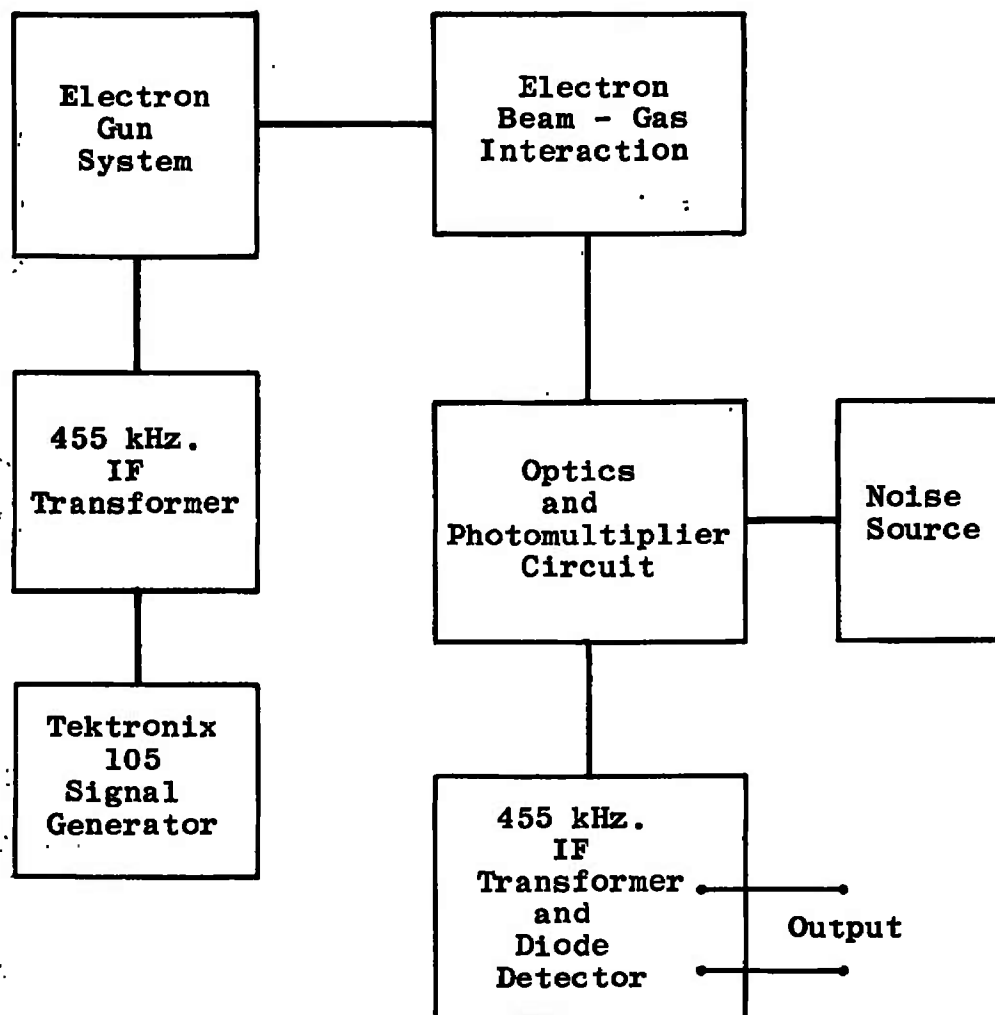versus noise frequency is shown in Figure 13, page 57.

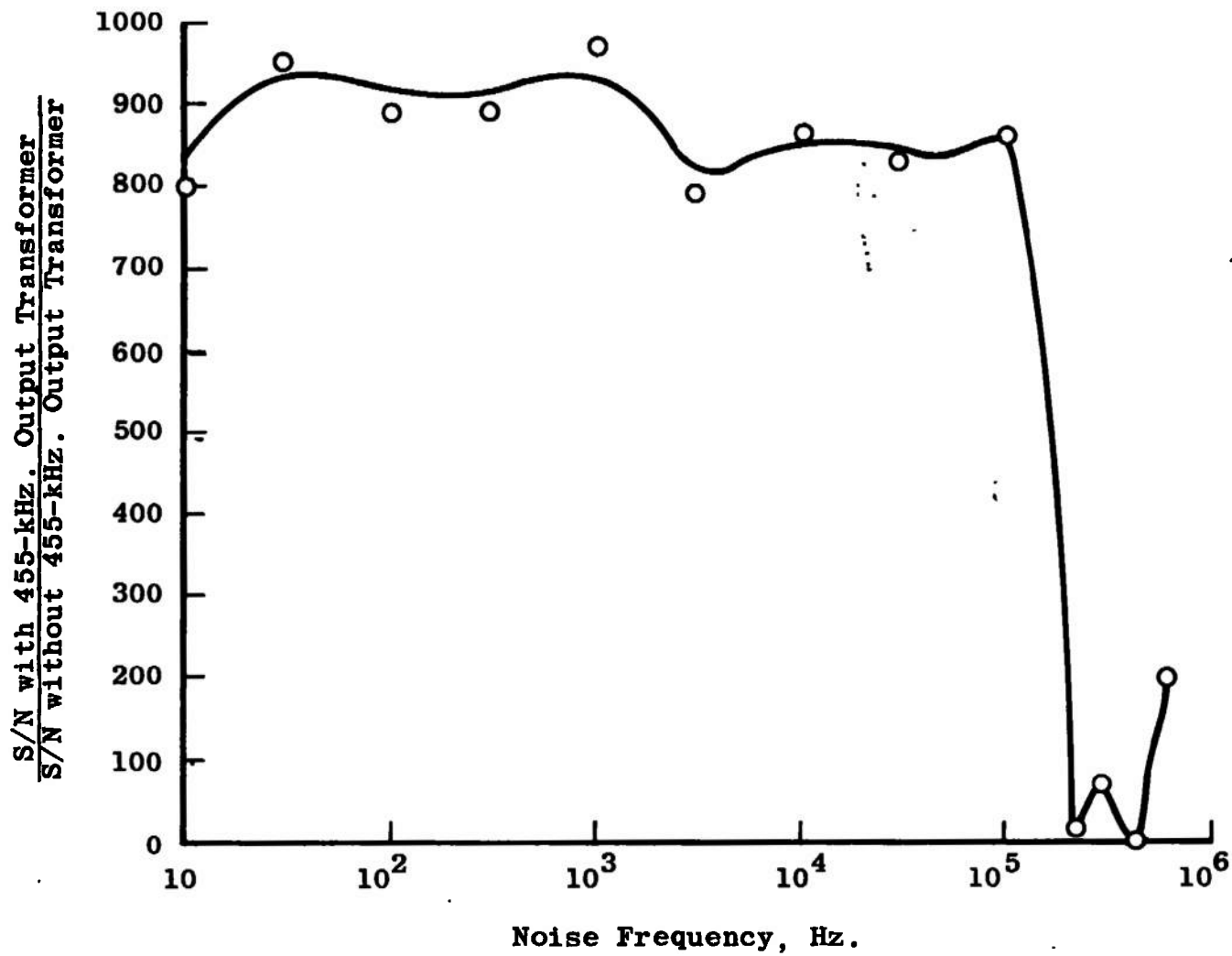Fig. 12 Amplitude Modulation and Detection System

Fig. 13. Amplitude Modulation and Detection System
Signal to Noise Ratio Improvement

DOCUMENT CONTROL DATA - R & D			
(Security classification of title, body of abstract and indexing annotation must be entered when the overall report is classified)			

1. ORIGINATING ACTIVITY *(Corporate author)*
Arnold Engineering Development Center,
ARO, Inc., Operating Contractor,
Arnold AF Station, Tennessee

2a. REPORT SECURITY CLASSIFICATION
UNCLASSIFIED

2b. GROUP
N/A

3. REPORT TITLE

DETERMINATION OF TRANSIENT GAS CONSTITUENT CONCENTRATIONS UTILIZING A HIGH ENERGY ELECTRON BEAM

4. DESCRIPTIVE NOTES *(Type of report and inclusive dates)*
November 1, 1966 to April 1, 1967 - Final Report

5. AUTHOR(S) *(First name, middle initial, last name)*

R. G. Whetsel, ARO, Inc.

6. REPORT DATE
May 1968

7a. TOTAL NO. OF PAGES
64

7b. NO. OF REFS
25

8a. CONTRACT OR GRANT NO. AF40(600)-1200

b. PROJECT NO. 7778

c. Program Element 6241003F

d. Task 777807

9a. ORIGINATOR'S REPORT NUMBER(S)

AEDC-TR-68-88

9b. OTHER REPORT NO(S) *(Any other numbers that may be assigned this report)*
N/A

10. DISTRIBUTION STATEMENT

This document has been approved for public release and sale; its distribution is unlimited.

11. SUPPLEMENTARY NOTES

Available in DDC.

12. SPONSORING MILITARY ACTIVITY
Arnold Engineering Development Center (AETS), Air Force Systems Command, Arnold AF Station, Tennessee

13. ABSTRACT

In order to determine the available test time in a helium driven shock tunnel, an interface detection system has been developed to indicate the arrival of helium driver gas at the test section. This is done by exciting the gas at the test section with a high energy electron beam and spectroscopically analyzing the resulting fluorescence to determine the helium concentration. Relative values of helium and air emission intensities are calculated and compared with experimental data from both static and transient gas mixtures.

DD FORM 1473
1 NOV 65

14. KEY WORDS	LINK A		LINK B		LINK C	
	ROLE	WT	ROLE	WT	ROLE	WT
gas constituents						
shock tunnels						
electron beams						
helium concentrations						
helium intensities						
air intensities						

3. Gases - Analysis

4 - 11